¹Selvin Prem Kumar S.
²Agees Kumar C.

Computer Aided Diagnosis of Brain Tumour Using Walrus Optimization Algorithm

JES

Journal of Electrical Systems

Abstract: - Brain tumour segmentation is one of the most challenging problems in medical image analysis. To detect brain cancers, radiologists must use a computer-based tumour classification model. In medical imaging research, several computer-aided diagnostic (CAD) models are available to help radiologists with their patients. The reason for brain growth division is to deliver exact outline of brain tumour regions. This study suggests a Walrus Optimisation Algorithm approach for detecting brain tumours using MRI (Magnetic Resonance Imaging). Separating the characteristics into four categories has been utilized: no growth, gliomas, meningiomas, and pituitary cancers. The deep learning based model inception AlexNet and ResNet-18 is trained on an augmented training dataset. The CNN classifier is used for characteristics map improvement, while the LSTM (Long momentary memory) classifier is utilized for order. Besides, the boundary remembered for the classifiers is chosen aimlessly utilizing the Walrus Improvement Calculation to build the presentation of the CNN-LSTM classifier. The performance of the tumour diagnosis is assessed using the metrics: overall classification accuracy of 98.8%, precision of 96.23%, recall of 97.01%, specificity of 98%.

Keywords: Computer-Aided Diagnosis (CAD), Walrus Optimization Algorithm (WOA), Deep Learning (DL), Magnetic Resonance Imaging (MRI), Long short-term memory (LSTM)

1. INTRODUCTION

In general, a brain tumour is a collection of abnormal brain cells. By and large, a cerebrum growth is an assortment of unusual synapses. uncontrollable cell division can raise intracranial tension, actually hurting ordinary mind structures. Mind growths that can obliterate brain tissues are among the most lethal ailments since the brain is perhaps of the most basic organ. Cerebrum cancers are liable for 3.24 passings per 100,000 individuals on normal [1]. Brain cancers must be correctly recognised at an early stage to increase patient survival. In many medical clinics, brain X-ray pictures are physically dissected. Nonetheless, radiologists should break down many pictures each day, which can prompt inaccurate diagnoses. There are two kinds of mind cancers: disease causing and non-carcinogenic, and the most well-known types of mind cancers relying upon the beset area are meningioma, glioma, and pituitary. Every one of these growths has an alternate measure of danger [2,3].

Glioma is a sort of frontal cortex dangerous development that makes on the neurons tissues and spinal string, meningioma is a kind of disease that makes on the film (the region that defends the psyche and spinal line), and pituitary development makes on the pituitary organ. It is one of the most generally utilized high-precision illness area and expressive procedures [4]. In any case, concluding the sickness type with X-beam is monotonous, obfuscated, and botch slanted, requiring the use of astoundingly gifted radiologists. Because

¹ Department of Computer Science and Engineering, CSI Institute of Technology, Thovalai, Tamil Nadu, India, selvincsiit@gmail.com

Department of EEE, Arunachala College of Engineering for Women, Nagercoil, Tamil Nadu, India, ageesofficials@gmail.com

tumours vary in appearance, observable characteristics in MRI images that aid in decision-making are not always present. As a result, people cannot rely on manual diagnosis [5].
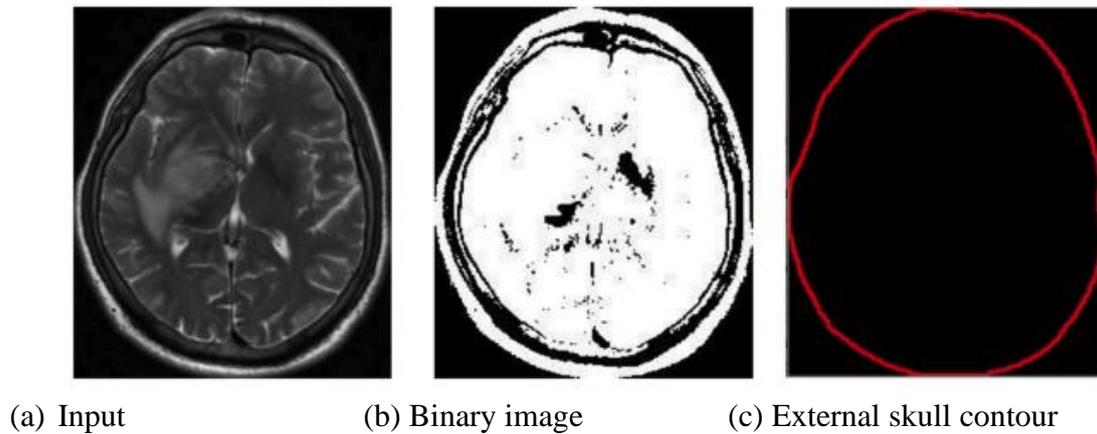

(a) Input   (b) Binary image   (c) External skull contour

Figure.1 Detecting the external skull contour

The brain is a significant organ in the human body since it oversees and manages the elements of the remainder of the body [6]. It is the focal sensory system's order and control focus, responsible for the human body's everyday deliberate and compulsory cycles. The cancer is a wild sinewy organization of unusual tissue development inside our brain [7]. Radiologists every now and again utilize attractive reverberation imaging (X-ray) to survey the phases of brain disease to forestall and fix the cancer. The discoveries of this exploration demonstrate the presence of a brain cancer. CNN utilize fractional differential capabilities to change over a complicated contribution to an enactment structure. Figure 1 depicts the technique for concluding the outside skull structure. The CNN setup is contained the layers which incorporates powerfully, the pooling layers test over the spatial region, and the totally related layer orchestrates [8,9]. A vanishing slant issue can happen when little numbers appear while handling tendencies. The data layer, dropout layer, yield layer, and association in network layer are the other CNN layers.

2. RELATED WORK

The computer aided design framework has exhibited promising outcomes in helping radiologists in diagnosing cerebrum growths quickly and precisely. The profound learning framework ResNet-50 CNN engineering might work on the distinguishing proof of cerebrum growths in X-ray information. The scientists had the option to recognize cerebrum malignant growths with 92.5% exactness in the wake of preparing the calculation on 700 X-ray brain images [10-12]. They utilized the ResNet-50 convolutional brain organization (CNN) design for include extraction and arrangement. The superb exactness of their computer aided design framework shows that it very well may be a significant device for radiologists in the early finding of cerebrum cancers, working on persistent results. Future exploration in this space could focus on the consolidation of computer aided design [13].

A few exploration have created PC helped identification (computer aided design) frameworks in light of MATLAB-based picture handling calculations for distinguishing mind cancers in X-ray information. For example, a PC supported plan system that disengaged illness regions from X-beam pictures including locale improvement and dynamic shape techniques.

The computer aided design framework accomplished growth division exactness of 94.6% [14]. This is same as a computer aided design method for recognizing cerebrum growths in light of element extraction from MATLAB information and backing vector machine order. They utilized MATLAB to separate visual attributes like power, surface, and shape prior to preparing a SVM classifier to recognize cancers. Their framework has a high exactness of 95.7% in distinguishing mind cancers, showing the need of MATLAB-based strategies for exact growth characterization [15].

Brain tumours are regarded as one of the most difficult medical research challenges due to their wide range of shape, size, and severity [16]. However profound learning calculations have created promising outcomes in PC supported finding lately, they actually have far to go. The most squeezing concerns are the advancement of further developed division procedures, modern component extraction and choice methodologies, and further developed order approaches [17-19]. Magnetic resonance imaging segmentation for brain tumours not only detects the growth but also provides a better description of the centre and decorative growth. A brain convolution-based approach utilizes Glioma Mind Cancer Division Organizations in Attractive Reverberation Imaging, and the cycle is a mixture of different Convolution Brain Organization models that utilization nearby and worldwide information on cerebrum tissue to foresee the name of every pixel, consequently further developing outcomes [20].

The following are the contributions of this paper:

In this review, an advanced deep learning based brain cancer order model is introduced which characterizes mind X-ray images into 4-classes as pituitary-growth, meningioma-growth, glioma-growth and no-cancer. The proposed model joins individual CNN and enhanced LSTM classifiers. The WOA algorithm is used to best decide the LSTM classifier to improve the organization's accuracy. The exhibition of the AlexNet and ResNet-18 profound learning models in the early distinguishing proof of brain tumour is explored and analyzed. A comparison with prior research is offered to validate the new model's improved classification accuracy.

This research is organised as follows. The first section gives an overview of the relevant studies for brain tumour identification. Section 2 contains a review of the literature. The proposed technique is detailed in Section 3. Section 4 explained the suggested method's performance measure. Section 5 summarises our findings and discussions. Finally, Section 6 brings our work to a close.

3. PROPOSED METHODOLOGY

Deep neural network learning strategies have been spread on a mission to fabricate the precision of assurance of grouped medical images and to help specialists and radiologists in the early acknowledgment of sicknesses. The Gaussian channel is utilized to diminish commotion. This channel smoothes pictures by diminishing the difference between neighboring pixels. To overcome the problems presented by conventional approaches, the suggested WOA-based deep convolution neural network is used to detect brain tumour patients from their tumours pictures, where statistical and textural information are taken to conduct the classification. Figure 2 depicts the suggested method's block diagram. For each MRI scan, a total of 9,216 characteristics are retrieved. As a result, the component map is 3060 (picture) 9216 (highlight) pixels in size. All photos are furthermore analyzed by SoftMax using profound

learning calculations for two models, AlexNet and ResNet-18. The LSTM classifier's performance is measured by its accuracy, sensitivity, recall, and specificity.
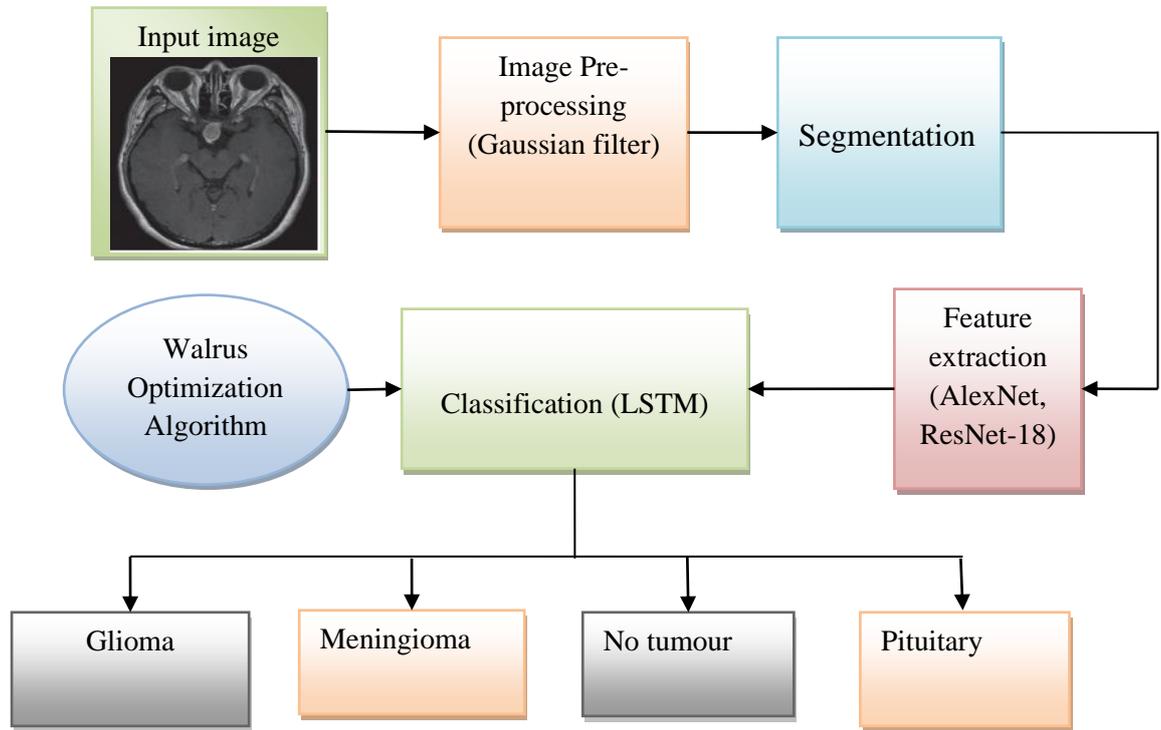

Figure.2 Block diagram of proposed method

Convolutional, pooling, and fully linked layers make up their overall design. Convolutional layers extract local differentiating characteristics by applying gaussian filters (3 3 and 5 5) to each input picture. These characteristics are passed on to the following layer. Institution maps, which choose the most useful features, stay aware of features. By reducing the picture viewpoints and cutting down the underlying cost, layer pooling decreases the size of the data picture and speeds up the action. The best not altogether settled by totally associated layers and ship off order layers, which execute the course of action connection considering the amount of classes.
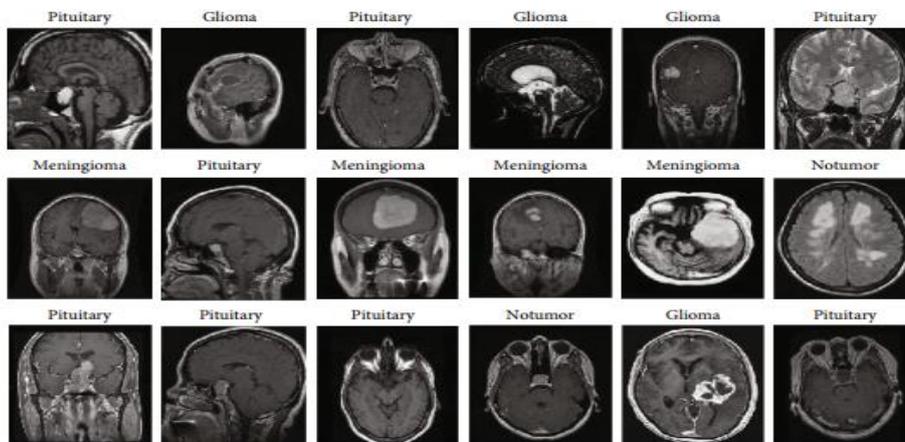

Figure.3 MRI brain tumours samples dataset

At last, profound CNN is utilized to recognize mind growths utilizing the component vector, with the profound CNN prepared utilizing the proposed WOA. The recommended WOA is expected to acquire the advantages of the two enhancements, bringing about powerful

classifier preparing.The brain tumour database is used to assess system performance. Figure 3 depicts samples from an MRI dataset of brain tumours. The dataset contains 3,060 MRI scans separated into four categories: 826 glioma photos, 937 meningioma images, 396 no_tumour images, and 901 pituitary tumour images. All MRI pictures are 512 512 pixels in size.

3.1 Image Pre-processing

The Gaussian channel is utilized to dispense the noise during the preprocessing step. The motivation behind pre-handling is to consider quicker handling of the approaching picture. Pre-handling is believed to be a significant stage in planning pictures for the recognizing system. Moreover, pre-handling is acted to eliminate the picture's noise and artifacts. Moreover, the pre-handling might be upheld as a picture upgrade module, which has the chance of expanding picture contrast for brain tumour identification. The pre-processed pictures are input into segmentation at the same time in order to identify important characteristics appropriate for brain cancer diagnosis.

3.2 Segmentation

To distinguish the tumour region from the other structures, it was hypothesised that pixels in the region must be contiguous with appropriate intensities. The item and the backdrop are split into two distinct groups with different grey scales in intensity-based thresholding. One of the easiest approaches for intensity-based thresholding is to use an image histogram that shows the grey scale distributions of the picture. The majority of thresholding methods utilised today are either semi-automatic or non-automatic.

3.3 Feature Extraction

The qualities of each and every development are then eliminated. deep learning has the benefit of figuring the convolutional layer. Convolutional, pooling, and completely associated layers are the three most significant layers in models. Convolutional layers are planned around three significant boundaries: channel size, insurance, and recurrence. Many channels are utilized in each layer to separate profound properties.

Table.1 Detailed structure of the ResNet-18 CNN

Layer	Conv1	Conv2x	Conv3x	Conv4x	Conv5x	Pooling
Output size	112*112*64	56*56*64	28*28*128	14*14*256	7*7*512	1*1*512
Filter	7*7, 64	3*3, 64 3*3, 64	3*3, 128 3*3, 128	3*3, 256 3*3, 256	3*3, 512 3*3, 512	Average

3.4 Classification

The LSTM furthermore utilizes an entryway configuration involved input, neglect, and output to refresh and deal with the framework's information execution. The LSTM routs the shortcomings of RNNs by settling the issue of point decline while overseeing long term information addictions through memory limit cells and entryway frameworks. The mathematical condition for each gate is made explained below.

$$F^t = \sigma\big(W_f[H^{t-1}, X^t] + B_f\big) \qquad (1)$$

Where H^{t-1} represent the previous gate,

$$C = \widetilde{tanh} (W_c[H^{t-1}, X^t] + B_c) \qquad (2)$$
$$I^t = \sigma(W_i[H^{t-1}, X^t] + B_i) \qquad (3)$$
$$C^t = F^t \times C^{t-1} + I^t \times \widetilde{C} \qquad (4)$$

The output gate O^t is then established to regulate the result of the LSTM cells. The expected result H^t is addressed by the blend of O^t and the cell state C^t set off by the tanh capability.

$$O^t = \sigma(W_o[H^{t-1}, X^t] + B_o) \qquad (5)$$
$$H^t = O^t.tanh\ tanh\ C^t \qquad (6)$$

Table 2 summarises the picture datasets that were used. The LSTMs model parameters are carefully set in order to restore the efficacy using the WOA method. CNN is used to extract the features, while LSTM is used to do the classification.

Table.2 Summary of used image dataset

Class	Number of images
Glioma	826
Meningioma	937
No tumour	396
Pituitary tumour	901

3.5 Walrus Optimization Algorithm (WOA)

The proposed WOA approach for identifying brain tumour is given, and the recognition is progressed using the component vector. The recovered highlights are accommodated order utilizing CNN, and the classifier is prepared utilizing the recommended WOA preparing strategy. The suggested WOA's purpose is to detect malignant spots from the input picture using the extracted characteristics. The goal is to determine the best parameter setup for CNN architectures. This arrangement will improve the accuracy of brain illness prediction while minimising function value loss. The proposed WOA improves the convergence rate to get the global optimal solution. It can tackle real-world problems with complex unknown search areas. Large, flip-flopped marine mammals, walruses inhabit the Arctic Ocean and the subarctic seas surrounding the North Pole in the Northern Hemisphere. The majority of gregarious walruses' time is spent on sea ice, where they search for food in the form of benthic bivalve mollusks.

The searcher members of this population in the population-based metaheuristic algorithm WOA are walruses. Every walrus in WOA stands for a potential fix for the optimisation issue. Initially, walrus populations are initialised at random when WOA is initially established. The WOA population matrix is calculated with the help of (7)

$$X = [X_1 .. X_i .. X_N]_{N \times M}$$
$$= \left[x_{1,1} … .. x_{i,1} .. x_{N,1} ….. x_{1,j} … .. x_{i,j} .. x_{N,j} …. x_{1,m} … .. x_{i,m} .. x_{N,m} ….. \right]_{N \times m} \qquad (7)$$

As recently shown, each walrus addresses a likely answer for the issue, and the goal capability of the issue might be surveyed in light of the qualities that it recommends for the decision factors. (8) specifies the walrus-derived goal function's estimated values.

$$F = [F_1 .. F_i .. F_N]_{N \times 1} = [F(X_1) .. F(X_i) .. F(X_N)]_{N \times 1} \qquad (8)$$

The objective function values are the best metric for evaluating the quality of proposed solutions. The best member is the candidate solution with the highest value assessment.

Phase 1: Feeding strategy (exploration)

Walruses are large, flip-flopped marine animals that live in the subarctic seas around the North Pole in the Northern Hemisphere and the Arctic Ocean. Gregarious walruses spend much of their time on the sea ice, where they look for benthic bivalve mollusks to eat. It uses its sensitive vibrissae and vigorous flipper movements to locate and discover food. The group's strongest and longest-tusked walrus leads the other walruses in their hunt for food. Different search space regions are scanned as a result of the walruses' activity, enhancing the EWaOA's capacity for exploration throughout the global search.Using equations (9) and (10), the feeding mechanism is used to quantitatively simulate the process by which walruses update their location, with the leader of the group serving as the guide. First, in accordance with (9), This operation results in the creation of a new position for Walrus. This new location takes the place of the previous one if it raises the value of the goal function; This concept is replicated in (10).

$$V_g = x_{i,j} + rand_{i,j}(SW_j - I_{i,j}.x_{i,j}) \quad (9)$$

$$I_q = \{x_i^{p_1}, F_i^{p_1} < F_i \, x_i, else,\} \quad (10)$$

Phase 2: Migration

Walruses travel to rocky beaches or outcrops as part of their usual habit as the temperature warms in the late summer. The WOA employs this migratory mechanism to help the walruses find appropriate locations inside the search space. According to this modelling, every walrus moves to a different (randomly chosen) location in a different part of the search space. As a result, the suggested new position, which takes the place of the Walrus position, increases the value of the goal function.

Phase 3: Escaping and fighting against predators (exploitation)

Killer whales and polar bears are constant threats to walruses. The walruses' position in relation to their current location changes as a result of their escape and defence tactics against these predators. In order to simulate this behaviour in WOA, each walrus is supposed to have a neighbourhood surrounding it, and each one is initially given a randomly generated new position inside this neighbourhood. The WOA flowchart is displayed in Figure 4.
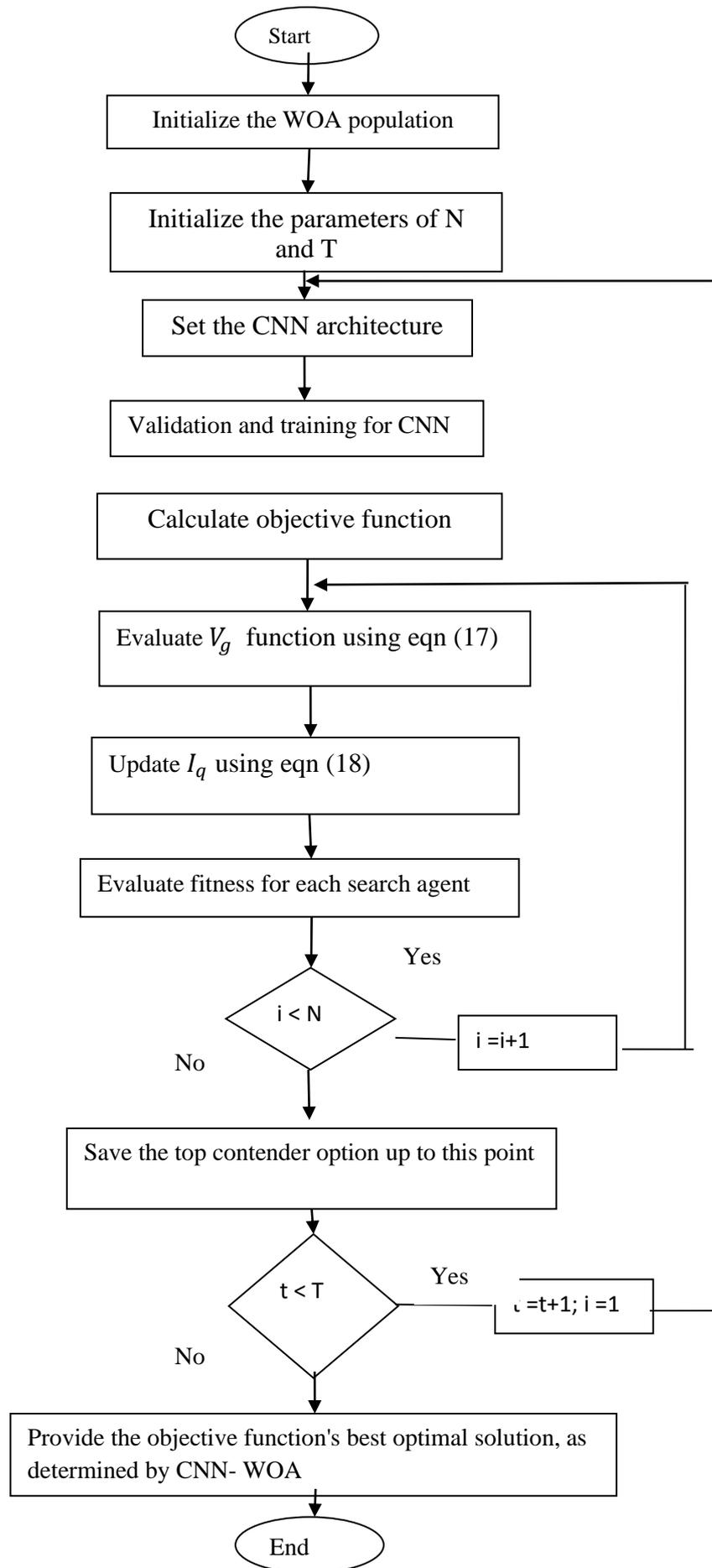
```
                        ┌─────────┐
                        │  Start  │
                        └────┬────┘
                             ▼
           ┌──────────────────────────────────┐
           │   Initialize the WOA population   │
           └────────────────┬─────────────────┘
                            ▼
           ┌──────────────────────────────────┐
           │   Initialize the parameters of N  │
           │              and T                │
           └────────────────┬─────────────────┘
                            ▼
           ┌──────────────────────────────────┐
           │      Set the CNN architecture     │
           └────────────────┬─────────────────┘
                            ▼
           ┌──────────────────────────────────┐
           │    Validation and training for CNN │
           └────────────────┬─────────────────┘
                            ▼
           ┌──────────────────────────────────┐
           │    Calculate objective function   │
           └────────────────┬─────────────────┘
                            ▼
```

- Start
- Initialize the WOA population
- Initialize the parameters of N and T
- Set the CNN architecture
- Validation and training for CNN
- Calculate objective function
- Evaluate V_g function using eqn (17)
- Update I_q using eqn (18)
- Evaluate fitness for each search agent

Decision: i < N
- Yes → i = i+1
- No ↓

Save the top contender option up to this point

Decision: t < T
- Yes → t = t+1; i = 1
- No ↓

Provide the objective function's best optimal solution, as determined by CNN- WOA

End

Figure.4 Flowchart of proposed WOA

4. PERFORMANCE MEASURE

(a) Image preprocessing:

The Peak Signal to Noise Ratio (PSNR) and Structural Similarity Index Measure (SSIM) were utilized as execution estimates in this examination.

The PSNR between a noisy image V size c×d and an input image U is defined as

$$PSNR = 10\left(\frac{255^2}{MSE(U,V)}\right) \qquad (11)$$

MSE stands for mean square error, which is represented as

$$MSE = \frac{1}{cd}\sum_{x=1}^{c}\sum_{y=1}^{d}\left(U_{xy} - V_{xy}\right) \qquad (12)$$

Where l_1 (U,V) - Luminance distortion

c_1(U,V) - Contrast comparison between two images

s_1(U,V) - Correlation coefficient between two images u and v

(b) Segmentation

The Jaccard and Dice similarity coefficient, which compared segmented output, is used to evaluate segmentation accuracy. The following formula is used to determine accuracy:

$$Jaccard\ (R,S) = \frac{|Intersection(R,S)|}{|Union(R,S)|} \quad (13)$$

(c) Brain Tumour Grade Classification Task

Various performance measures are typically used to assess primary classifiers. The majority of these attributes are, however, generated from four fundamental decision scores. True Positive (TP), True Negative (TN), False Positive (FP), and False Negative (FN) are among these ratings. The percentage of patients who are accurately diagnosed is measured by the ACC (accuracy). The CNN-WOA networks' training settings and hyper parameters are employed, and test data is used to assess how well they perform.

$$Accuracy = \frac{t_p + t_n}{t_p + t_n + f_p + f_n} \times 100 \quad (14)$$

$$Precision = \frac{t_p}{f_p + t_p} \qquad (15)$$

$$Recall = \frac{t_p}{f_n + t_p} \qquad (16)$$

$$Specificity = \frac{t_n}{f_p + t_n} \quad (17)$$

The following definitions apply to the true positive (TPR) and negative rates (TNR):

$$TPR = \frac{TP}{TP + FN} \qquad (18)$$

$$TNR = \frac{TN}{TN + FP} \qquad (19)$$

The sensitivity, recall, and hit rate are all other names for the TPR score. The terms "true negative" and "specificity" are used to describe the TNR score. The best performance metric, accuracy, is used to evaluate the suggested strategy's effectiveness. Accuracy, sensitivity, Recall and specificity are performance assessment criteria that are used infrequently

for the identification and classification of brain tumour. TP is characterized as, forecast as a malignant growth and is really a disease.

● Forecasting as a cancer is what FP is actually: a normal.
● TN is defined as a normal prediction that is actually a normal.
● FN is characterized as, expectation as an ordinary and is very disease.

5. SIMULATION RESULTS

In this research, MATLAB2021a is utilized to execute the proposed strategy on Intel(R) core (TM) i7-6500U central processor at 2.50GHz 2.60 GHz. Numerous assessment have been circulated to check out at the show of existing estimate computations. Following the consummation of the pre-handling, the part assurance extraction is finished, followed by the request. In the principal stage, a CNN is joined with a WOA estimation to remove and pick the most prominent features from the information planning dataset. In this work, only one X-ray dataset of a cerebrum cancer is utilized to prepare CNN, with the leftover datasets used to assess the model's exhibition.
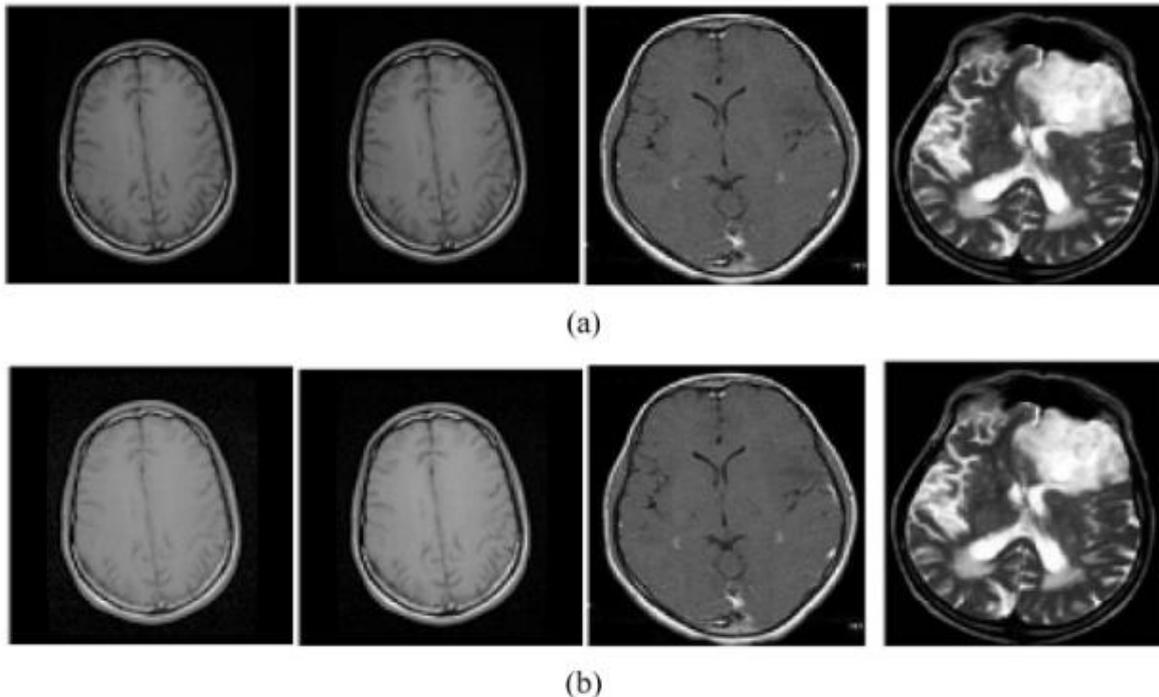

(a)

(b)

Fig.5 Results of pre-processing (a) Input image and (b) Pre-processed image.

Alexnet and inception V3 pre-prepared models accept a picture as info and lead a few stages like convolution, surveying, completely associated, and ultimately SoftMax to produce characterization results. Figure 5 portrays the pre-handling results (a) input picture and (b) pre-handled picture. Two CNN models, AlexNet and ResNet-18, were utilized to analyze X-ray pictures from a mind growth dataset.
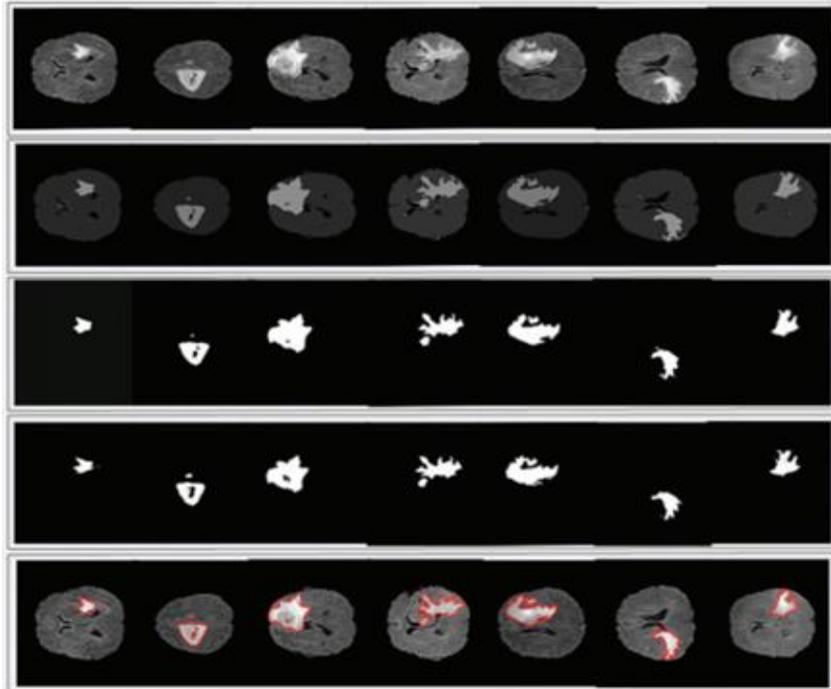
Figure.6 segmentation results of proposed work

Figure 6 depicted a comparison of suggested segmentation work with dataset ground truth pictures. The correctly categorised photographs were TP and TN, whereas the wrongly classified ones were FP and FN. Accuracy, sensitivity, recall, and specificity are all important considerations. In terms of accuracy, sensitivity, recall, and specificity, the models provided promising results. The crossover procedure was picked because of multiple factors, the most significant of which was to accomplish promising demonstrative exactness when contrasted.

Table.3 Accuracy for each tumour diagnostic

Tumour type	ResNet-18	AlexNet	ResNet-18+LSTM	AlexNet+ LSTM
Glioma	92.42	92.67	92.65	94.84
Meningioma	88.67	92.81	92.92	93.57
Pituitary	96.23	96.45	97.23	97.98
No tumour	90.43	86.76	93.10	95.72
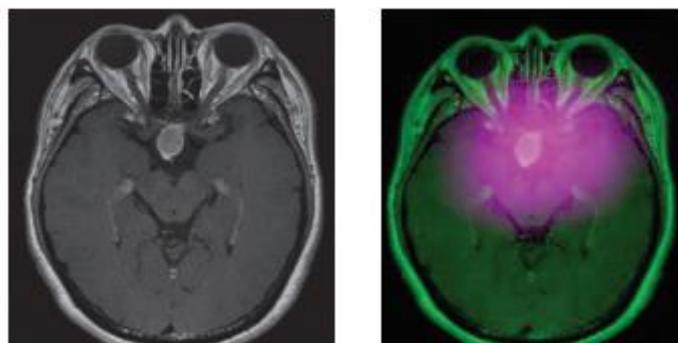
(a) Input image   (b) Activation of the tumour

Fig.7 Activation of tumour area (Neon pink color) in the CNN-WOA

The features obtained from the first convolution layer and deeper layer are used to activate the tumour area. The activated feature may take values 0 –less activation and 1- highest activation. The activation is further represented as (a) white pixel- strong positive activation (b) grey pixel- no activation and (c) black pixel- strong negative activation. In the proposed work tumour area activation is best analyzed in convolution layers. The strongest positive activation is merged on the input testing data, to evaluate the tumour activated area is shown in figure 7.
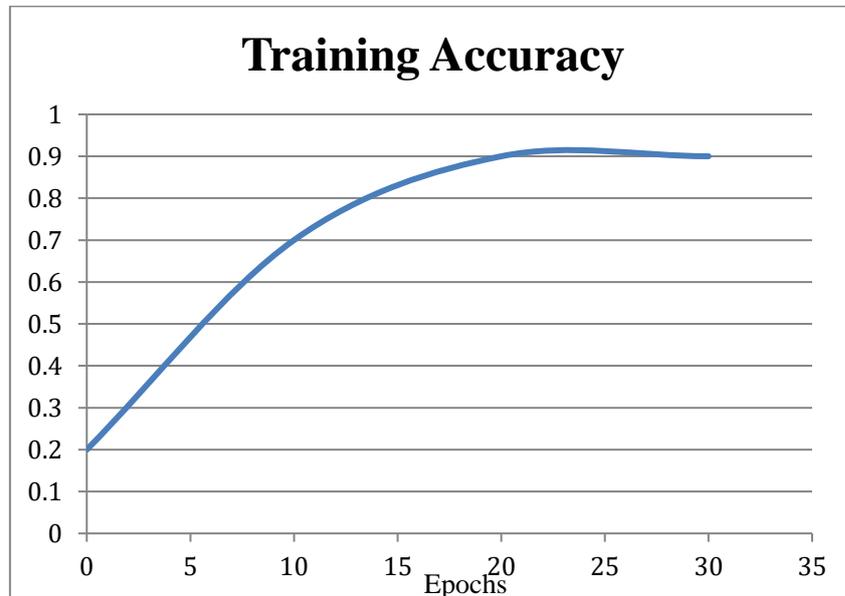

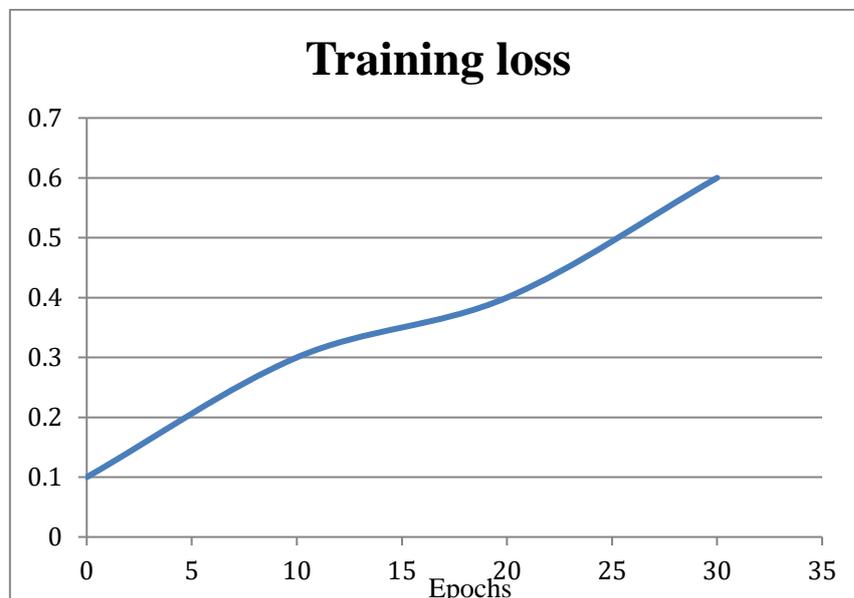**Figure.8** Training accuracy per epoch

Figure.9 Training loss per epoch

Table 3 compares about the precision of analysis of the four strategies for every tumour class. The best glioma assurance accuracy achieved with the AlexNet+LSTM cross variety model is 94.84%, while the best meningioma indicative precision achieved with a comparative model is 93.57%. The AlexNet+LSTM hybrid model achieves the highest diagnosis accuracy of nontumor pictures (95.72%). Table 4 depicts a classification method performance measure.

The AlexNet+LSTM hybrid model has the highest diagnosis accuracy for pituitary tumours at 97.98%. Figures 8 and 9 depict the graphical depiction of accuracy and loss during model training, respectively.

Table.4 Performance measures of classification method

Evaluation Metrics	CNN-WOA
Accuracy	98.8%
Precision	96.23%
Recall	97.01%
Specificity	98%

Table.5 Performance comparison of various existing methods with the proposed method

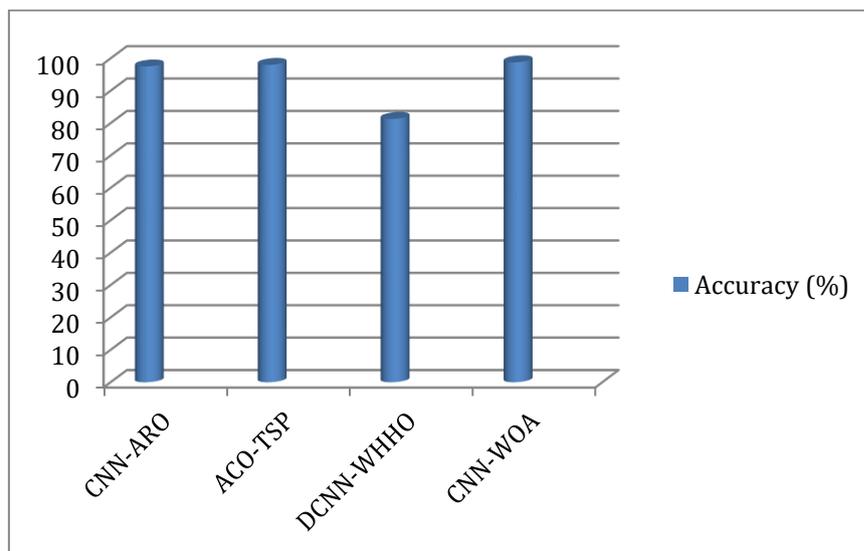| Authors	Methods	Accuracy (%)
S. Shanthi (2022) [25]	CNN- ARO	97.5
Kamel.H (2019) [20]	ACO-TSP	98.0
D. Rammurthy (2022) [23]	DCNN-WHHO	81.3
Proposed	CNN-WOA	98.8

Figure.10 Comparison of proposed CNN-WOA and other methods

Accuracy, recall, precision, and specificity are used to determine the detection performance. Figure 10 shows the performance comparison of CNN-ARO, ACO-TSP, and DCNN-WHHO with different algorithms. Table 5 compares the performance of several current approaches to the suggested method. By achieving greater accuracy as compared to the CNN-

WOA approach, the proposed method performed better. The proposed method achieved 98.8% accuracy and the existing methods are achieved 97.5% by S. Shanthi et al. (2022) [25], 98.0% by Kamel.H (2019) [20], 81.3% by D. Rammurthy (2022) [23].

CONCLUSION

The detection of a brain tumour is troublesome because of the multifaceted the human body of the brain. The brain is responsible for coordinating the elements of the body's all's organs. Deep learning algorithms for automated categorization of early-stage brain tumours play a significant role. The proposed model combines individual CNN and optimised LSTM classifiers. The WOA algorithm is used to best choose the LSTM classifier to boost the organization's accuracy. We directed four preliminaries to analyze three types of cerebrum growths (meningioma, glioma, and pituitary) and one sound picture class utilizing X-ray pictures. The pictures were improved utilizing the Gaussian channel. Deep learning models were utilized to remove profound and isolating qualities from the improved photographs. Deep learning highlights were recognized utilizing SoftMax CNN classifiers and LSTM profound learning classifiers utilizing WOA techniques. All of the suggested systems produced encouraging results for identifying brain cancers from MRI scans, with no variation in accuracy between models. Among different models, the AlexNet+LSTM mixture model played out the best. It accomplished accuracy, sensitivity,recall and specificity of 98.8%, 96.23%, 97.01, and 98%, individually.

REFERENCES
[1] Huang, Zheng, Han Xu, Shun Su, Tianyu Wang, Yang Luo, Xingang Zhao, Yunhui Liu, Guoli Song, and Yiwen Zhao. "A computer-aided diagnosis system for brain magnetic resonance imaging images using a novel differential feature neural network." Computers in biology and medicine 121 (2020): 103818.
[2] Alqudah, Ali Mohammad, Hiam Alquraan, Isam Abu Qasmieh, Amin Alqudah, and Wafaa Al-Sharu. "Brain tumor classification using deep learning technique--a comparison between cropped, uncropped, and segmented lesion images with different sizes." arXiv preprint arXiv:2001.08844 (2020).
[3] Senan, Ebrahim Mohammed, Mukti E. Jadhav, Taha H. Rassem, Abdulaziz Salamah Aljaloud, Badiea Abdulkarem Mohammed, and Zeyad Ghaleb Al-Mekhlafi. "Early diagnosis of brain tumour mri images using hybrid techniques between deep and machine learning." Computational and Mathematical Methods in Medicine 2022 (2022).
[4] Brindha, P. Gokila, M. Kavinraj, P. Manivasakam, and P. Prasanth. "Brain tumor detection from MRI images using deep learning techniques." In IOP conference series: materials science and engineering, vol. 1055, no. 1, p. 012115. IOP Publishing, 2021.
[5] Regev, Ohad et al. "Tumor-Treating Fields for the treatment of glioblastoma: a systematic review and meta-analysis." Neuro-oncology practice vol. 8,4 426-440. 20 Apr. 2021, doi:10.1093/nop/npab026.
[6] Naseer, Asma, Tahreem Yasir, Arifah Azhar, Tanzeela Shakeel, and Kashif Zafar. "Computer-aided brain tumor diagnosis: performance evaluation of deep learner CNN using augmented brain MRI." International Journal of Biomedical Imaging 2021 (2021).

[7] El-Dahshan, El-Sayed A., Heba M. Mohsen, Kenneth Revett, and Abdel-Badeeh M. Salem. "Computer-aided diagnosis of human brain tumor through MRI: A survey and a new algorithm." Expert systems with Applications 41, no. 11 (2014): 5526-5545.

[8] Alhothali, Abdullah, Ali Samkari, and Umar S. Alqasemi. "Enhanced System for Computer-Aided Detection of MRI Brain Tumors." International Journal of Advanced Computer Science and Applications 14, no. 10 (2023).

[9] Henry T, Carre A, Lerousseau M, Estienne T, Robert C, Paragios N, Deutsch E (2020) Brain tumor segmentation with selfensembled, deeply-supervised 3d u-net neural networks: a brats 2020 challenge solution

[10] Alhothali, Abdullah, Ali Samkari, and Umar S. Alqasemi. "Enhanced System for Computer-Aided Detection of MRI Brain Tumors." International Journal of Advanced Computer Science and Applications 14, no. 10 (2023).

[11] Jeyalakshmi et al., "CAD system for brain tumor classification using MATLAB-based feature extraction and support vector machine," 2019.

[12] Rinesh, S., K. Maheswari, B. Arthi, P. Sherubha, A. Vijay, S. Sridhar, T. Rajendran, and Yosef Asrat Waji. "Investigations on brain tumor classification using hybrid machine learning algorithms." Journal of Healthcare Engineering 2022 (2022).

[13] Kadhim, Yezi Ali, Muhammad Umer Khan, and Alok Mishra. "Deep learning-based computer-aided diagnosis (cad): applications for medical image datasets." Sensors 22, no. 22 (2022): 8999.

[14] Sandhiya, B., and S. Kanaga Suba Raja. "Deep Learning and Optimized Learning Machine for Brain Tumor Classification." Biomedical Signal Processing and Control 89 (2024): 105778.

[15] Kang, Jaeyong, Zahid Ullah, and Jeonghwan Gwak. "Mri-based brain tumor classification using ensemble of deep features and machine learning classifiers." Sensors 21, no. 6 (2021): 2222.

[16] Rehman, Arshia, Saeeda Naz, Muhammad Imran Razzak, Faiza Akram, and Muhammad Imran. "A deep learning-based framework for automatic brain tumors classification using transfer learning." Circuits, Systems, and Signal Processing 39 (2020): 757-775.

[17] Díaz-Pernas, Francisco Javier, Mario Martínez-Zarzuela, Míriam Antón-Rodríguez, and David González-Ortega. "A deep learning approach for brain tumor classification and segmentation using a multiscale convolutional neural network." In Healthcare, vol. 9, no. 2, p. 153. MDPI, 2021.

[18] Gürkahraman, Kali, and R. U. K. İ. Y. E. Karakiş. "Brain tumors classification with deep learning using data augmentation." Journal of the Faculty of Engineering and Architecture of Gazi University 36, no. 2 (2021): 997-1011.

[19] Musallam, Ahmed S., Ahmed S. Sherif, and Mohamed K. Hussein. "A new convolutional neural network architecture for automatic detection of brain tumors in magnetic resonance imaging images." IEEE access 10 (2022): 2775-2782.

[20] Aly, Rabab Hamed M., Kamel H. Rahouma, and Hesham FA Hamed. "Brain tumors diagnosis and prediction based on applying the learning metaheuristic optimization techniques of particle swarm, ant colony and bee colony." Procedia Computer Science 163 (2019): 165-179.

[21] Huang, Zhiguan, Xiaohao Du, Liangming Chen, Yuhe Li, Mei Liu, Yao Chou, and Long Jin. "Convolutional neural network based on complex networks for brain tumor image classification with a modified activation function." IEEE Access 8 (2020): 89281-89290.

[22] Asif, Sohaib, Wenhui Yi, Qurrat Ul Ain, Jin Hou, Tao Yi, and Jinhai Si. "Improving effectiveness of different deep transfer learning-based models for detecting brain tumors from MR images." IEEE Access 10 (2022): 34716-34730.

[23] Rammurthy, D., and P. K. Mahesh. "Whale Harris hawks optimization based deep learning classifier for brain tumor detection using MRI images." Journal of King Saud University-Computer and Information Sciences 34, no. 6 (2022): 3259-3272.

[24] Rizwan, Muhammad, Aysha Shabbir, Abdul Rehman Javed, Maryam Shabbir, Thar Baker, and Dhiya Al-Jumeily Obe. "Brain tumor and glioma grade classification using Gaussian convolutional neural network." IEEE Access 10 (2022): 29731-29740.

[25] Shanthi, S., S. Saradha, J. A. Smitha, N. Prasath, and H. Anandakumar. "An efficient automatic brain tumor classification using optimized hybrid deep neural network." International Journal of Intelligent Networks 3 (2022): 188-196.